17

Pythagorean–hodograph Curves

> *If the velocity vector of a particle is translated so as to start from the center of force, then the heads of the vectors trace out the particle's hodograph, a locus of considerable antiquity in the history of mechanics.*
>
> H. Goldstein, *Classical Mechanics* [213]

The hodograph of a parametric curve $\mathbf{r}(t)$ in $\mathbb{R}^n$ is just its derivative $\mathbf{r}'(t)$, regarded as a parametric curve in its own right. A polynomial curve $\mathbf{r}(t)$ in $\mathbb{R}^n$ is a *Pythagorean–hodograph* (PH) *curve* if the n coordinate components of its hodograph are elements of a Pythagorean $(n+1)$–tuple of polynomials — i.e., the sum of their squares coincides with the square of another polynomial $\sigma(t)$. Pythagorean–hodograph curves in $\mathbb{R}^2$ and $\mathbb{R}^3$ entail quite different approaches to their characterization, since Pythagorean polynomial triples and quartuples involve disparate algebraic structures. We are concerned here with just planar PH curves, and defer the treatment of spatial PH curves to Part V. A further extension, concerning PH curve formulations in Minkowski space $\mathbb{R}^{n,1}$ with n space–like and one time–like coordinates, is addressed in Chap. 24.

The definition, elementary properties, and Bernstein–Bézier representation of planar PH curves are presented below, exclusively in terms real variables. In Chap. 19 an alternative formulation is defined in terms of complex variables: the elegance and economy of expression this offers ensures its use as the basis for subsequent planar PH curve algorithms, such as construction of Hermite interpolants (Chap. 25), computation of the elastic bending energy integral (Chap. 26), and solution of the C^2 spline equations (Chap. 27).

17.1 Planar Pythagorean Hodographs

The key property that distinguishes a planar PH curve $\mathbf{r}(t) = (x(t), y(t))$ from an "ordinary" polynomial curve is the *a priori* incorporation of a Pythagorean structure in its hodograph — namely, the components of $\mathbf{r}'(t) = (x'(t), y'(t))$ are required to satisfy the condition

$$x'^2(t) + y'^2(t) = \sigma^2(t) \tag{17.1}$$

for some polynomial $\sigma(t)$. This property is achieved by invoking the following characterization for Pythagorean triples of polynomials.

Theorem 17.1 *The Pythagorean condition*

$$a^2(t) + b^2(t) = c^2(t) \tag{17.2}$$

is satisfied by polynomials $a(t)$, $b(t)$, $c(t)$ if and only if they can be expressed in terms of other polynomials $u(t)$, $v(t)$, $w(t)$ in the form

$$\begin{aligned} a(t) &= \left[\, u^2(t) - v^2(t) \,\right] w(t) \,, \\ b(t) &= 2u(t)v(t)w(t) \,, \\ c(t) &= \left[\, u^2(t) + v^2(t) \,\right] w(t) \,, \end{aligned} \tag{17.3}$$

where $u(t)$ and $v(t)$ are relatively prime.

Proof : That the form (17.3) is a *sufficient* condition for satisfaction of (17.2) follows immediately from substitution into this equation. To see that it is also *necessary*,[1] set $w(t) = \gcd(a(t), b(t), c(t))$ and consider the polynomials

$$\tilde{a}(t) = \frac{a(t)}{w(t)} \,, \qquad \tilde{b}(t) = \frac{b(t)}{w(t)} \,, \qquad \tilde{c}(t) = \frac{c(t)}{w(t)} \,,$$

which are relatively prime and satisfy

$$\tilde{a}^2(t) + \tilde{b}^2(t) = \tilde{c}^2(t)$$

if $a(t)$, $b(t)$, $c(t)$ are a Pythagorean triple satisfying (17.2). Re–writing this as

$$\tilde{b}^2(t) = \tilde{c}^2(t) - \tilde{a}^2(t) = [\, \tilde{c}(t) + \tilde{a}(t) \,] \, [\, \tilde{c}(t) - \tilde{a}(t) \,] \,,$$

we note that $\tilde{c}(t) + \tilde{a}(t)$ and $\tilde{c}(t) - \tilde{a}(t)$ can have no common roots, since the existence of such roots would imply common roots of $\tilde{a}(t)$, $\tilde{b}(t)$, $\tilde{c}(t)$. Hence, every root of $\tilde{b}(t)$ must be a root of *either* $\tilde{c}(t) + \tilde{a}(t)$ *or* $\tilde{c}(t) - \tilde{a}(t)$, of *even* multiplicity, and without loss of generality we may write

$$\tilde{c}(t) + \tilde{a}(t) = 2\,u^2(t) \qquad \text{and} \qquad \tilde{c}(t) - \tilde{a}(t) = 2\,v^2(t)$$

for relatively prime polynomials $u(t)$ and $v(t)$, such that $\tilde{b}^2(t) = 4\,u^2(t)v^2(t)$. From these three equations, we may deduce that

$$\tilde{a}(t) = u^2(t) - v^2(t) \,, \quad \tilde{b}(t) = 2u(t)v(t) \,, \quad \tilde{c}(t) = u^2(t) + v^2(t) \,,$$

and multiplying through by $w(t)$ yields the stated form (17.3). ∎

---

[1] This argument is adapted from the well–known proof for integer Pythagorean triples: see, for example, [95]. For a more general proof, in the context of unique factorization domains of characteristic not equal to 2, see [292].

Remark 17.1 One can easily verify that solutions with $\gcd(a(t),b(t),c(t)) =$ constant correspond to taking $w(t) =$ constant and $\gcd(u(t),v(t)) =$ constant in (17.3). Such solutions are called *primitive* Pythagorean triples.

Thus, a planar PH curve $\mathbf{r}(t) = (x(t),y(t))$ is defined by substituting three polynomials $u(t)$, $v(t)$, $w(t)$ into the expressions

$$x'(t) \,=\, [\,u^2(t) - v^2(t)\,]w(t)\,, \qquad y'(t) \,=\, 2u(t)v(t)w(t) \tag{17.4}$$

and integrating. There is no loss of generality in identifying $x'(t)$ and $y'(t)$ with $a(t)$ and $b(t)$, respectively, in Theorem 17.1 — as noted in §2.2, alternatives to the polynomials $u(t)$ and $v(t)$ can always be obtained to satisfy the converse identification. Also, we assume in (17.4) that $u(t)$ and $v(t)$ are *relatively prime* — i.e., $\gcd(u(t),v(t)) =$ constant — since any non–constant common factor of $u(t)$ and $v(t)$ can be absorbed in $w(t)$. We must also discount certain choices for $w(t)$, $u(t)$, $v(t)$ that yield "degenerate" PH curves:

(a) if $w(t) = 0$ or $u(t) = v(t) = 0$, the resulting hodograph $x'(t) = y'(t) = 0$ defines a *single point* rather than a continuous locus;
(b) if $w(t)$, $u(t)$, $v(t)$ are all constants (with w and at least one of u, v non–zero) we obtain a uniformly–parameterized *straight line*, a trivial PH curve;
(c) if $u(t)$ and $v(t)$ are constants, not both zero, and $w(t)$ is not a constant, the locus obtained by integrating (17.4) is again linear but its *parametric speed* is non–uniform — in general, it is *multiply–traced* over intervals delineated by odd–multiplicity roots of $w(t)$;
(d) non–uniformly parameterized linear loci (parallel to the x–axis) also arise if $w(t) \neq 0$ and one of $u(t)$ and $v(t)$ is zero.

Henceforth we shall consider only cases where $w(t)$, $u(t)$, $v(t)$ are all non–zero, and $u(t)$, $v(t)$ are not *both* constants.

Remark 17.2 If $\lambda = \deg(w(t))$ and $\mu = \max(\deg(u(t)),\deg(v(t))$, the PH curve obtained by integrating the hodograph (17.4) is of degree $n = \lambda + 2\mu + 1$.

Lemma 17.1 *PH curves of degree n have at most $n+3$ degrees of freedom, as compared to the $2(n+1)$ degrees of freedom associated with general polynomial curves of degree n.*

Proof : If $\mu = \max(\deg(u(t),v(t))$ the polynomials $u(t)$, $v(t)$ are each specified by at most $\mu+1$ coefficients. If $\lambda = \deg(w(t))$ we associate only λ coefficients with $w(t)$, since without loss of generality we may assume its leading coefficient is unity. Hence, we may freely choose $\lambda + 2(\mu+1)$ coefficients when specifying $u(t)$, $v(t)$, $w(t)$ and the integration constants provide two further freedoms, yielding a total of $\lambda + 2\mu + 4 = n + 3$ by the preceding remark. ∎

However, these freedoms are not all available for manipulating the *intrinsic shape* of PH curves. Three of them are accounted for by choosing the origin and orientation of the coordinate axes, and another two correspond to freedoms of parameterization — since the substitution $t \to at + b$ does not alter the shape or degree of the curve. Discounting these, we see that PH curves of degree n have $n-2$ "shape freedoms" while general polynomial curves have $2n-3$.

17.2 Bézier Control Points of PH Curves

We focus here primarily on hodographs of the form (17.4) with $w(t) = 1$ and $\gcd(u(t), v(t)) = \text{constant}$ — i.e., the *primitive* Pythagorean hodographs. Such hodographs define *regular* PH curves, satisfying $\mathbf{r}'(t) \neq \mathbf{0}$ for all t. A point on a parametric curve where $\mathbf{r}'(t)$ vanishes is a non–regular point — typically, a *cusp* or sudden tangent reversal. The use of a non–constant polynomial $w(t)$ in (17.4) incurs cusps (an undesirable feature) on the corresponding PH curve if $w(t)$ has real roots within the curve parameter domain. PH curves defined by integrating primitive hodographs are of *odd* degree, $n = 2\mu + 1$.

The simplest non–trivial PH curves arise from substituting $w(t) = 1$ and linear Bernstein–form polynomials

$$u(t) \,=\, u_0\, b_0^1(t) \,+\, u_1\, b_1^1(t)\,, \quad v(t) \,=\, v_0\, b_0^1(t) \,+\, v_1\, b_1^1(t)$$

satisfying $u_0 v_1 - u_1 v_0 \neq 0$ and $(u_1 - u_0)^2 + (v_1 - v_0)^2 \neq 0$, so that $u(t)$, $v(t)$ are relatively prime and not both constants, into (17.4) to obtain the hodograph

$$\begin{aligned} x'(t) \,&=\, (u_0^2 - v_0^2)\, b_0^2(t) \,+\, (u_0 u_1 - v_0 v_1)\, b_1^2(t) \,+\, (u_1^2 - v_1^2)\, b_2^2(t)\,, \\ y'(t) \,&=\, 2u_0 v_0\, b_0^2(t) \,+\, (u_0 v_1 + u_1 v_0)\, b_1^2(t) \,+\, 2u_1 v_1\, b_2^2(t)\,. \end{aligned}$$

Integrating this hodograph using (11.7) then yields a PH cubic with Bézier control points of the form

$$\begin{aligned} \mathbf{p}_1 \,&=\, \mathbf{p}_0 + \frac{1}{3}\left(u_0^2 - v_0^2, 2u_0 v_0\right)\,, \\ \mathbf{p}_2 \,&=\, \mathbf{p}_1 + \frac{1}{3}\left(u_0 u_1 - v_0 v_1, u_0 v_1 + u_1 v_0\right)\,, \\ \mathbf{p}_3 \,&=\, \mathbf{p}_2 + \frac{1}{3}\left(u_1^2 - v_1^2, 2u_1 v_1\right)\,, \end{aligned} \tag{17.5}$$

the control point $\mathbf{p}_0$, defined by the integration constants, being freely chosen.

Control polygons of the form (17.5) can also be characterized by intuitive geometrical constraints, that we derive in Chap. 18. Now according to the discussion of §17.1 the PH cubics possess just one "shape freedom," and we show in Chap. 18 that this amounts to simply a *uniform scaling*. Hence, if we discount scaling as well as translation, rotation, and re–parameterization, the PH cubics are all segments of a *unique* curve, known (among other names) as *Tschirnhausen's cubic*. A complete analysis of this curve, and a discussion of its many interesting properties, is deferred to Chap. 18.

Clearly, PH cubics are of limited value for free–form curve design due to their minimal shape flexibility — although a method for constructing Hermite interpolants using "double" PH cubics (i.e., pairs of PH cubic segments with G^1 junctures) was described in [179]. From expressions (17.16) below we note that the curvature of PH cubic segments cannot change sign, i.e., they cannot exhibit inflections (since $uv' - u'v$ is simply a constant if $u(t)$, $v(t)$ are linear). If we desire shape freedoms comparable to those of "ordinary" cubics, with a true inflectional capability, we must appeal to *quintic* PH curves.

To define quintic PH curves, we choose quadratic polynomials

$$u(t) \;=\; u_0\, b_0^2(t) \;+\; u_1\, b_1^2(t) \;+\; u_2 b_2^2(t)\,, \quad v(t) \;=\; v_0\, b_0^2(t) \;+\; v_1\, b_1^2(t) \;+\; v_2\, b_2^2(t)$$

in (17.4) and integrate, to obtain Bézier control points of the form

$$\begin{aligned}
\mathbf{p}_1 \;&=\; \mathbf{p}_0 + \frac{1}{5}(u_0^2 - v_0^2, 2u_0v_0)\,, \\
\mathbf{p}_2 \;&=\; \mathbf{p}_1 + \frac{1}{5}(u_0u_1 - v_0v_1, u_0v_1 + u_1v_0)\,, \\
\mathbf{p}_3 \;&=\; \mathbf{p}_2 + \frac{2}{15}(u_1^2 - v_1^2, 2u_1v_1) + \frac{1}{15}(u_0u_2 - v_0v_2, u_0v_2 + u_2v_0)\,, \\
\mathbf{p}_4 \;&=\; \mathbf{p}_3 + \frac{1}{5}(u_1u_2 - v_1v_2, u_1v_2 + u_2v_1)\,, \\
\mathbf{p}_5 \;&=\; \mathbf{p}_4 + \frac{1}{5}(u_2^2 - v_2^2, 2u_2v_2)\,,
\end{aligned} \tag{17.6}$$

where $\mathbf{p}_0$ is again arbitrary. In this case, the condition for $u(t)$ and $v(t)$ to be relatively prime may be phrased as

$$(u_2v_0 - u_0v_2)^2 \;\neq\; 4(u_0v_1 - u_1v_0)(u_1v_2 - u_2v_1)\,. \tag{17.7}$$

The PH quintics are in many respects analogous to the "ordinary" cubics — they may change their sense of curvature, and are capable of interpolating arbitrary first-order Hermite data, as described in Chap. 25. They are also the basic components of C^2 PH splines (see Chap. 27).

Lemma 17.2 *The PH quintic defined by* (17.6) *has either two real inflections or none, according to whether the quantity*

$$\Delta \;=\; (u_2v_0 - u_0v_2)^2 - 4\,(u_0v_1 - u_1v_0)\,(u_1v_2 - u_2v_1) \tag{17.8}$$

is positive or negative.

Proof : Substituting $u(t)$, $v(t)$ into the numerator $k(t) = u(t)v'(t) - u'(t)v(t)$ of expression (17.16) below for the curvature, $k(t)$ is seen to be the quadratic with Bernstein coefficients

$$k_0 = 2(u_0v_1 - u_1v_0)\,, \quad k_1 = -\,(u_2v_0 - u_0v_2)\,, \quad k_2 = 2(u_1v_2 - u_2v_1)\,.$$

Its discriminant $k_1^2 - k_0k_2$ is proportional to (17.8), and we observe that $\Delta \neq 0$ by virtue of the constraint (17.7). Thus, if $\Delta > 0$ there are two real t values for which κ vanishes, while if $\Delta < 0$ there are none. ∎

The control point formulae (17.5) and (17.6) characterize PH cubics and quintics in terms of the coefficients of the two *real* polynomials $u(t)$ and $v(t)$. A significant economy of expression can be realized by interpreting them as the real and imaginary parts of a single *complex* polynomial, $\mathbf{w}(t) = u(t) + \mathrm{i}\, v(t)$. This approach is developed in Chap. 19, and used extensively thereafter.

17.3 Parametric Speed and Arc Length

The parametric speed of a regular PH curve $\mathbf{r}(t) = (x(t), y(t))$ is given by

$$\sigma(t) \;=\; |\mathbf{r}'(t)| \;=\; \sqrt{x'^2(t) + y'^2(t)} \;=\; u^2(t) + v^2(t)\,, \tag{17.9}$$

a *polynomial* in t. If $\mathbf{r}(t)$ is of (odd) degree n, $u(t)$ and $v(t)$ must be of degree $m = \frac{1}{2}(n-1)$ and may be written in Bernstein form as

$$u(t) \;=\; \sum_{k=0}^{m} u_k b_k^m(t)\,, \qquad v(t) \;=\; \sum_{k=0}^{m} v_k b_k^m(t)\,.$$

To express (17.9) in the Bernstein form

$$\sigma(t) \;=\; \sum_{k=0}^{n-1} \sigma_k b_k^{n-1}(t)\,, \tag{17.10}$$

we invoke the multiplication rule (11.20) for Bernstein–form polynomials. This gives the coefficients of $\sigma(t)$ in terms of the coefficients of $u(t)$, $v(t)$ as

$$\sigma_k \;=\; \sum_{j=\max(0,k-m)}^{\min(m,k)} \frac{\binom{m}{j}\binom{m}{k-j}}{\binom{n-1}{k}} \, (u_j u_{k-j} + v_j v_{k-j})\,, \quad k = 0, \ldots, n-1\,.$$

For the PH cubics, for example, $\sigma(t)$ is quadratic and has Bernstein coefficients

$$\sigma_0 \;=\; u_0^2 + v_0^2\,, \qquad \sigma_1 \;=\; u_0 u_1 + v_0 v_1\,, \qquad \sigma_2 \;=\; u_1^2 + v_1^2\,, \tag{17.11}$$

while for the PH quintics, $\sigma(t)$ is the quartic with Bernstein coefficients

$$\begin{aligned}
\sigma_0 \;&=\; u_0^2 + v_0^2\,, \qquad \sigma_1 \;=\; u_0 u_1 + v_0 v_1\,, \\
\sigma_2 \;&=\; \frac{2}{3}\left(u_1^2 + v_1^2\right) + \frac{1}{3}\left(u_0 u_2 + v_0 v_2\right)\,, \\
\sigma_3 \;&=\; u_1 u_2 + v_1 v_2\,, \qquad \sigma_4 \;=\; u_2^2 + v_2^2\,.
\end{aligned} \tag{17.12}$$

In order to integrate $\sigma(t)$ and thus obtain the arc length s as a polynomial function of the parameter,

$$s(t) \,=\, \int_0^t \sigma(\tau)\,\mathrm{d}\tau\,,$$

we use the integration rule (11.7) for the Bernstein basis functions. This gives

$$s(t) \,=\, \sum_{k=0}^{n} s_k \binom{n}{k}(1-t)^{n-k}t^k\,, \tag{17.13}$$

where

$$s_0 \,=\, 0 \qquad \text{and} \qquad s_k \,=\, \frac{1}{n}\sum_{j=0}^{k-1}\sigma_j\,, \quad k=1,\ldots,n\,.$$

Hence, the total arc length S is simply

$$S \,=\, s(1) \,=\, \frac{\sigma_0+\sigma_1+\cdots+\sigma_{n-1}}{n}\,. \tag{17.14}$$

To compute the arc length of any PH curve segment $t \in [\,a,b\,]$ we need only take the difference $s(b)-s(a)$ of the polynomial (17.13) evaluated at a, b. The result is *exact* (modulo round–off errors if floating–point arithmetic is used), as distinct from arc length computations for “ordinary” polynomial curves — which require an inherently approximate numerical quadrature.

Similarly, it is much simpler to determine from (17.13) the parameter value t_* at which the arc length (measured from $t=0$) has a given value s_* — i.e., to solve the equation

$$s(t_*) \,=\, s_*$$

for t_*. Consider, for example, the task of *uniform rendering* of a parametric curve. Typically, $\mathbf{r}(t)$ is rendered by evaluating at parameter values $t_0,\ldots,t_N$ corresponding to a uniform parameter increment $\Delta t = t_k - t_{k-1}$, $k=1,\ldots,N$. However, this yields an uneven spacing (by arc length) of the points $\mathbf{r}(t_k)$ on the curve, since the parametric speed $\sigma(t)$ is not, in general, constant.

Although the parametric speed of a PH curve is also non–constant, the simple form (17.13) of $s(t)$ allows us to easily compensate for its variation. Let $t_0,\ldots,t_N$ be the parameter values of the points uniformly spaced by an arc–length increment $\Delta s = S/N$, so that

$$s(t_k) \,=\, k\,\Delta s\,, \qquad k=1,\ldots,N-1 \tag{17.15}$$

with $t_0=0$ and $t_N=1$. Now since $\sigma(t)=ds/dt$ and $\sigma(t)$ is positive for all t when $\mathrm{GCD}(u,v)=1$, $s(t)$ is *monotone–increasing* with t, and hence for each k equation (17.15) has precisely one simple real root. Clearly, the root t_k of (17.15) lies between t_{k-1} and 1. As an initial approximation to it, we take

$$t_k^{(0)} \,=\, t_{k-1} \,+\, \frac{\Delta s}{\sigma(t_{k-1})}$$

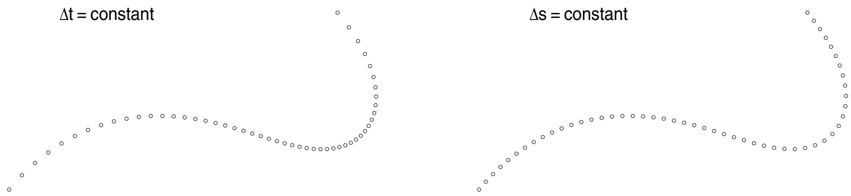

Fig. 17.1. Uniform increments in PH curve parameter (left) and arc length (right).

and obtain further refinements by applying the Newton–Raphson iteration

$$t_k^{(r)} \,=\, t_k^{(r-1)} \,-\, \frac{s(t_k^{(r-1)})}{\sigma(t_k^{(r-1)})}\,, \qquad r = 1, 2, \ldots\,.$$

As is well known [110], such iterations are *quadratically convergent* for starting approximations sufficiently close to t_k, and in typical examples the parameter values t_k are obtained to an accuracy of 10^{-12} or better in just two or three iterations (see Fig. 17.1) . Since *precise* uniformity by arc length is probably not crucial in many applications, a single iteration often suffices — typically, this gives uniform spacing to a relative accuracy of about 10^{-6} or better.

The problem of uniform arc–length rendering of a curve arises naturally in considering motion at *uniform speed* along a curve. This is the simplest case of a broader class of problems addressed by *real–time interpolator* algorithms for digital motion controllers. A comprehensive discussion of these problems, and the advantages of PH curves in solving them, can be found in Chap. 29.

17.4 Differential and Integral Properties

Since the parametric speed of the PH curve $\mathbf{r}(t)$ defined by integrating (17.4) is the *polynomial* (17.9) in t, its elementary differential properties — the unit tangent and normal, and the curvature — all have a *rational* dependence on the curve parameter. Specifically, they are defined in terms of the polynomials $u(t)$ and $v(t)$ by

$$\mathbf{t} \,=\, \frac{(u^2 - v^2, 2uv)}{\sigma}\,, \quad \mathbf{n} \,=\, \frac{(2uv, v^2 - u^2)}{\sigma}\,, \quad \kappa \,=\, 2\,\frac{uv' - u'v}{\sigma^2}\,. \tag{17.16}$$

For a degree–n PH curve, $\mathbf{t}$ and $\mathbf{n}$ are rational functions of degree $n-1$, while κ is of degree $n-3$ in the numerator and $2n-2$ in the denominator.

The fact that the unit normal $\mathbf{n}(t)$ is a rational vector function on a PH curve $\mathbf{r}(t)$ means that its offsets $\mathbf{r}_d(t)$ at each distance d are *rational curves* — they admit exact representations in the standard rational Bézier form of CAD systems (see §17.5), eliminating the need for data–intensive and error–prone offset curve approximation schemes [140, 251, 252, 280, 362].

The rational curvature function is another advantage of PH curves over "ordinary" polynomial curves, since integrals of powers of the curvature with respect to the arc length $\mathrm{d}s = \sigma\,\mathrm{d}t$, defined by

$$I_n \,=\, \int_0^1 \kappa^n(t)\,\sigma(t)\,\mathrm{d}t \qquad \text{for } n = 0, 1, 2, \ldots\,, \tag{17.17}$$

can be evaluated exactly by a partial fraction decomposition of the integrand (see §3.5). The case $n = 0$ gives the total arc length, discussed in §17.3 above. Since $\kappa = \mathrm{d}\theta/\mathrm{d}s$, where θ is the tangent angle with respect to a fixed direction, the integral I_1 defines the *net* rotation angle (i.e., with anti–clockwise rotation cancelling clockwise rotation) of the tangent along the curve. A modified form of I_1 is analyzed in §25.3, with $|\kappa|$ substituted for κ, defining the total *absolute* tangent rotation — this requires a subdivision of the parameter domain $[\,0,1\,]$ at the t values that identify inflection points of the PH curve.

Finally, the integral I_2 is the *bending energy* of the curve — i.e., the strain energy stored in a thin, initially straight, elastic beam that is bent into the shape of the curve (see §14.2). Chapter 26 addresses the evaluation of I_2 for PH curves in detail. Note that evaluation of the integrals (17.17) by means of partial fraction decomposition requires a factorization of the parametric speed polynomial. Since, by construction, $\sigma(t)$ has no real roots, this factorization involves only terms that correspond to complex–conjugate root pairs (which may be combined into real quadratic factors).

17.5 Rational Offsets of PH Curves

The offsets at each distance d from a PH curve $\mathbf{r}(t)$, defined by

$$\mathbf{r}_d(t) \,=\, \mathbf{r}(t) \,+\, d\,\mathbf{n}(t)\,, \tag{17.18}$$

admit *exact* representation as rational Bézier curves, because the unit normal $\mathbf{n}(t)$ has a rational dependence on the curve parameter t. In the case of cubics and quintics, the offset curves are of degree five and nine, respectively. Let the control points of the PH curve $\mathbf{r}(t)$ be written in homogeneous coordinates as

$$\mathbf{P}_k \,=\, (W_k, X_k, Y_k) \,=\, (1, x_k, y_k)\,, \quad k = 0, \ldots, n\,.$$

We define the forward differences of these coordinates by

$$\Delta\mathbf{P}_k \,=\, \mathbf{P}_{k+1} - \mathbf{P}_k \,=\, (0, \Delta x_k, \Delta y_k)\,, \quad k = 0, \ldots, n-1$$

where $\Delta x_k = x_{k+1} - x_k$, $\Delta y_k = y_{k+1} - y_k$, and we set $\Delta\mathbf{P}_k^{\perp} = (0, \Delta y_k, -\Delta x_k)$.

The offset at distance d from the PH curve $\mathbf{r}(t)$ is defined by (17.18), where the normal to $\mathbf{r}(t)$ is given by (17.16). The offset can be expressed as

$$\mathbf{r}_d(t) \,=\, \left(\frac{X(t)}{W(t)}, \frac{Y(t)}{W(t)}\right)$$

where $W(t)$, $X(t)$, $Y(t)$ are polynomials of degree $2n-1$, whose coefficients

$$\mathbf{O}_k \,=\, (W_k, X_k, Y_k)\,, \quad k = 0, \ldots, 2n-1$$

define the Bézier control points of the rational offset curve.

The homogeneous coordinates for the control points of the offset may be concisely expressed in terms of those of the original curve [148, 186] as

$$\mathbf{O}_k \,=\, \sum_{j=\max(0,k-n)}^{\min(n-1,k)} \frac{\binom{n-1}{j}\binom{n}{k-j}}{\binom{2n-1}{k}} (\sigma_j \mathbf{P}_{k-j} + d\, n \varDelta\mathbf{P}_j^{\perp})\,, \quad k = 0, \ldots, 2n-1\,.$$

Thus, for PH cubics, the control points of the rational quintic offsets are

$$\begin{aligned}
\mathbf{O}_0 &= \sigma_0 \mathbf{P}_0 + 3d\, \varDelta\mathbf{P}_0^{\perp}\,, \\
\mathbf{O}_1 &= \frac{1}{5}\,[\,2\sigma_1 \mathbf{P}_0 + 3\sigma_0 \mathbf{P}_1 + 3d\,(3\varDelta\mathbf{P}_0^{\perp} + 2\varDelta\mathbf{P}_1^{\perp})\,]\,, \\
\mathbf{O}_2 &= \frac{1}{10}\,[\,\sigma_2 \mathbf{P}_0 + 6\sigma_1 \mathbf{P}_1 + 3\sigma_0 \mathbf{P}_2 + 3d\,(3\varDelta\mathbf{P}_0^{\perp} + 6\varDelta\mathbf{P}_1^{\perp} + \varDelta\mathbf{P}_2^{\perp})\,]\,, \\
\mathbf{O}_3 &= \frac{1}{10}\,[\,3\sigma_2 \mathbf{P}_1 + 6\sigma_1 \mathbf{P}_2 + \sigma_0 \mathbf{P}_3 + 3d\,(\varDelta\mathbf{P}_0^{\perp} + 6\varDelta\mathbf{P}_1^{\perp} + 3\varDelta\mathbf{P}_2^{\perp})\,]\,, \\
\mathbf{O}_4 &= \frac{1}{5}\,[\,3\sigma_2 \mathbf{P}_2 + 2\sigma_1 \mathbf{P}_3 + 3d\,(2\varDelta\mathbf{P}_1^{\perp} + 3\varDelta\mathbf{P}_2^{\perp})\,]\,, \\
\mathbf{O}_5 &= \sigma_2 \mathbf{P}_3 + 3d\, \varDelta\mathbf{P}_2^{\perp}\,.
\end{aligned}$$

For PH quintics, the rational offsets are of degree 9 with control points

$$\begin{aligned}
\mathbf{O}_0 &= \sigma_0 \mathbf{P}_0 + 5d\, \varDelta\mathbf{P}_0^{\perp}\,, \\
\mathbf{O}_1 &= \frac{1}{9}\,[\,4\sigma_1 \mathbf{P}_0 + 5\sigma_0 \mathbf{P}_1 + 5d\,(5\varDelta\mathbf{P}_0^{\perp} + 4\varDelta\mathbf{P}_1^{\perp})\,]\,, \\
\mathbf{O}_2 &= \frac{1}{18}\,[\,3\sigma_2 \mathbf{P}_0 + 10\sigma_1 \mathbf{P}_1 + 5\sigma_0 \mathbf{P}_2 + 5d\,(5\varDelta\mathbf{P}_0^{\perp} + 10\varDelta\mathbf{P}_1^{\perp} + 3\varDelta\mathbf{P}_2^{\perp})\,]\,, \\
\mathbf{O}_3 &= \frac{1}{42}\,[\,2\sigma_3 \mathbf{P}_0 + 15\sigma_2 \mathbf{P}_1 + 20\sigma_1 \mathbf{P}_2 + 5\sigma_0 \mathbf{P}_3 \\
&\qquad + 5d\,(5\varDelta\mathbf{P}_0^{\perp} + 20\varDelta\mathbf{P}_1^{\perp} + 15\varDelta\mathbf{P}_2^{\perp} + 2\varDelta\mathbf{P}_3^{\perp})\,]\,, \\
\mathbf{O}_4 &= \frac{1}{126}\,[\,\sigma_4 \mathbf{P}_0 + 20\sigma_3 \mathbf{P}_1 + 60\sigma_2 \mathbf{P}_2 + 40\sigma_1 \mathbf{P}_3 + 5\sigma_0 \mathbf{P}_4 \\
&\qquad + 5d\,(5\varDelta\mathbf{P}_0^{\perp} + 40\varDelta\mathbf{P}_1^{\perp} + 60\varDelta\mathbf{P}_2^{\perp} + 20\varDelta\mathbf{P}_3^{\perp} + \varDelta\mathbf{P}_4^{\perp})\,]\,, \\
\mathbf{O}_5 &= \frac{1}{126}\,[\,5\sigma_4 \mathbf{P}_1 + 40\sigma_3 \mathbf{P}_2 + 60\sigma_2 \mathbf{P}_3 + 20\sigma_1 \mathbf{P}_4 + \sigma_0 \mathbf{P}_5 \\
&\qquad + 5d\,(\varDelta\mathbf{P}_0^{\perp} + 20\varDelta\mathbf{P}_1^{\perp} + 60\varDelta\mathbf{P}_2^{\perp} + 40\varDelta\mathbf{P}_3^{\perp} + 5\varDelta\mathbf{P}_4^{\perp})\,]\,,
\end{aligned}$$

$$
\begin{aligned}
\mathbf{O}_6 &= \frac{1}{42}\,[\,5\sigma_4\mathbf{P}_2 + 20\sigma_3\mathbf{P}_3 + 15\sigma_2\mathbf{P}_4 + 2\sigma_1\mathbf{P}_5 \\
&\qquad + 5d\,(2\Delta\mathbf{P}_1^\perp + 15\Delta\mathbf{P}_2^\perp + 20\Delta\mathbf{P}_3^\perp + 5\Delta\mathbf{P}_4^\perp)\,]\,, \\
\mathbf{O}_7 &= \frac{1}{18}\,[\,5\sigma_4\mathbf{P}_3 + 10\sigma_3\mathbf{P}_4 + 3\sigma_2\mathbf{P}_5 + 5d\,(3\Delta\mathbf{P}_2^\perp + 10\Delta\mathbf{P}_3^\perp + 5\Delta\mathbf{P}_4^\perp)\,]\,, \\
\mathbf{O}_8 &= \frac{1}{9}\,[\,5\sigma_4\mathbf{P}_4 + 4\sigma_3\mathbf{P}_5 + 5d\,(4\Delta\mathbf{P}_3^\perp + 5\Delta\mathbf{P}_4^\perp)\,]\,, \\
\mathbf{O}_9 &= \sigma_4\mathbf{P}_5 + 5d\,\Delta\mathbf{P}_4^\perp\,.
\end{aligned}
$$

Figure 17.2 illustrates the control polygons specified by the above formulae, and the offset curves they define, for some PH quintics. Since the offsets are *rational* curves (each control point having, in general, a different weight W_k) the control polygons of the offsets are not necessarily intuitive indicators of the shape of the curves they define. Figure 17.3 shows that, as d increases, the offset curve control points move uniformly along straight lines.

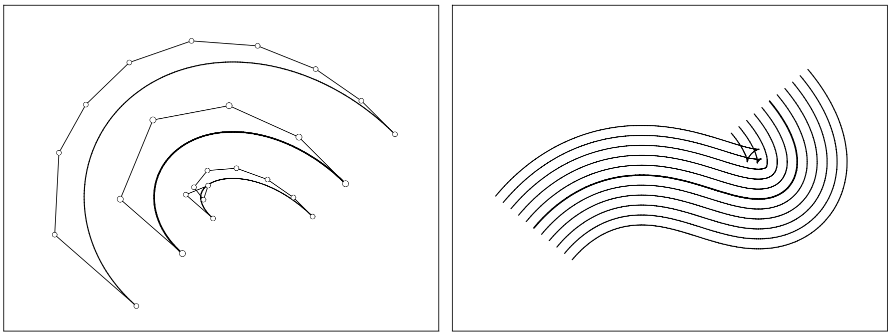

Fig. 17.2. Left: Bézier control polygons for degree 9 interior and exterior offsets to a PH quintic (note that each control point has a different weight). Right: the rational offsets are exact for every d — even when they develop cusps and self–intersections.

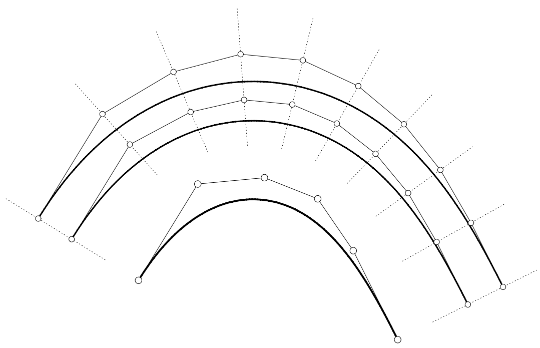

Fig. 17.3. Control polygons for offsets at two different distances d from a PH quintic: as d increases, the offset control points move uniformly along certain straight lines.